Desalination and Water Treatment
www.deswater.com

doi: 10.1080/19443994.2015.1020514

57 (2016) 8561–8574
April

Taylor & Francis
Taylor & Francis Group

Kinetic and adsorption study of Pb (II) toward different treated activated carbons derived from olive cake wastes

Ahmed A. El-Kady[a,*], Robert Carleer[b], Jan Yperman[b], Jan D'Haen[c], Hany H. Abdel Ghafar[d,e,1]

[a]*Food Toxicology & Contaminants Department, National Research Centre, Cairo, Egypt, Tel. +20 122 8809386; Fax: +202 333 70 931; email: aelkady16@gmail.com*
[b]*Research Group of Applied and Analytical Chemistry, CMK, Universiteit Hasselt, Agoralaan, Building D, BE-3590 Diepenbeek, Belgium, Tel. +32 011 26 83 58; email: robert.carleer@uhasselt.be (R. Carleer), Tel. +32 011 26 83 20; email: jan.yperman@uhasselt.be (J. Yperman)*
[c]*Institute for Materials Research & IMEC-associated lab IMOMEC, Universiteit Hasselt, Wetenschapspark 1, BE-3590 Diepenbeek, Belgium, email: jan.dhaen@uhasselt.be*
[d]*Faculty of Science and Arts, Department of Chemistry, King Abdulaziz University, Khulais, Saudi Arabia, Tel. +20 2 333 71 479; email: hany_ghafar@hotmail.com*
[e]*Water Pollution Department, National Research Centre, Cairo, Egypt*

Received 12 October 2014; Accepted 11 February 2015

ABSTRACT

Adsorption capacity of activated carbons (ACs) derived from olive cake toward Pb (II) was tested in batch single ion experimental mode as a function of time, pH, carbon dose, and initial ion concentration. Physicochemical properties were carried out for produced ACs and a commercial Organosorb 10-CO to elucidate the variations of observed results. The total pore volume reached 0.676 $cm^3 g^{-1}$ for AC2 (activated under forced air); however, AC1 (activated under nitrogen) and Organosorb 10-CO had almost similar total pore volume (0.448 and 0.432 $cm^3 g^{-1}$, respectively). The mesopore volume for AC2 was 2.5 and 50 times of AC1 and Organosorb 10-CO, respectively. The scanning electron microscope images reflect the enhancement of thermochemical activation by H_3PO_4 in increasing the porosity of both ACs. The adsorption of lead ions onto the ACs (confirmed by energy dispersive X-ray) occurred rapidly, since 45 and 48% of lead ions were adsorbed within 30 min onto AC1 and AC2, respectively, in contrast to a limited uptake for Organosorb 10-CO (27%). The $q_{\max}$ was achieved within 2 h for AC1 and AC2; however, 3 h was required for Organosorb 10-CO. The tablet form of the commercial AC performs much slower in lead adsorption but established a much higher lead removal percent than the granular form. Langmuir isotherm provided the best fit to the equilibrium data with maximum adsorption capacity of 58.14, 188.67, and 39.84 $mg g^{-1}$ for AC1, AC2, and Organosorb 10-CO, respectively. The sorption energy (E-value) was 19.36, 8.92, and 11.48 $kJ mol^{-1}$ for AC1, AC2, and Organosorb 10-CO, respectively, which indicated that the adsorption process takes physically place.

---

*Corresponding author.

[1] Faculty of Science and Arts-Khulais, Department of Chemistry, University of Jeddah, Jeddah, Saudi Arabia, Tel. +996 53364 5049.

Keywords: Activated carbon; Lead; Abatement and removal; Olive cake; New form

1. Introduction

Lead is a nonessential element that occurs naturally in the environment. However, the highest concentrations found in nature are the result of human activities. Based on its physical and chemical properties, such as softness, malleability, ductility, poor conductibility, and resistance to corrosion, man uses lead and lead compounds (e.g. lead acetate, lead nitrate, and lead oxide) for a great variety of applications [1,2]. Drinking water is the major source of lead, estimated to be responsible for approximately 20% of the total daily exposure [3]. Lead poisoning has been recognized as a major public health risk and affecting children, especially poor children in developing countries [4]. The lead permissible limit in drinking water and surface water intended for drinking set by European Union, USEPA, and WHO is 0.010, 0.015, and 0.010 mg l^{-1} [5,6]. The agency for toxic substances and disease registry and the environmental protection agency (EPA) stated that there is no toxic threshold for lead. This means there is no measurable level of lead in the body below which no harm occurs. Therefore, EPA has listed a maximum contaminant level goal of 0 μg l^{-1} for lead in water [7]. So, research efforts dealing with the process affecting the removal or reducing the level of lead ions in environmental media are urgently needed. Among the classical wastewater treatments, bio-sorption of trace metals is an alternative technique, primarily because it utilizes inactive/dead biological materials as sorbents which are generally available at low cost, nonhazardous, and abundant in nature [8–10]. The use of organic by-products for the preparation of activated carbons (ACs) is very attractive due to their contribution for decreasing costs of waste disposal, widely available. In addition, ACs were used as adsorbent materials because of their extended surface area (500–1,500 m^2 g^{-1}), microporous structure, high adsorption capacity, and high degree of surface reactivity [11–13]. Furthermore, the presence of different surface functional groups on ACs, especially oxygen groups, leads to the adsorption of trace metals ions [14].

From the almost 3.3 million tones of olive oils estimated by International Olive Council to be produced in the world during 2011/2012, 97% comes from the Mediterranean region. In Egypt, the land under olive cultivation has expanded dramatically over the last three decades, increasing 19-folds from 3,700 in 1980 to approximately 65,303 ha in 2009. Table 1 represented the progress of olive oils & table olive production in Egypt throughout the last two decades [15].

The extraction of olive oil generates huge quantities of wastes that may have a great impact on land and water environments because of their high phytotoxicity [16]. Several studies have proven the negative effects of these wastes on soil microbial populations [17], on aquatic ecosystems [18], and even in air medium [19]. It is expected to face environmental problems associated with the huge amounts of solid wastes coming from the crude olive cake composed of olive pulp and olive stone. Consequently, olive cake was chosen for more than one reason. In addition to its abundance, it is robust and stable, and it does not swell in aqueous media [20].

On the other hand, the main problems associated with the use of regular ACs in water treatment are: (i) the preparation cost of ACs and (ii) the cost of ACs separation from aqueous media after treatment on a pilot scale. In order to overcome these problems, ACs should be prepared from waste materials to decrease the production cost and should be applied to water treatment in easily separated forms.

Two types of ACs derived from olive cake wastes were tested for their potential applications in sequestration of lead ions from aqueous solution under different conditions.

A crucial point of our targets was also to study the differences between ACs which were activated under nitrogen flow and forced air. In addition, commercial AC was also tested in a tablet form to be easily separated from the aqueous lead ion solution. Physicochemical properties were investigated for produced ACs and a commercial Organosorb 10-CO to elucidate the variations of observed results.

2. Materials & methods

2.1. Materials and reagents

Phosphoric acid (85%) and lead standard solutions of 1,000 mg l^{-1} used for preparation of working solution and for inductively coupled plasma atomic emission spectroscopy (ICP-AES) calibration were purchased from Merck, Darmstadt, Germany. Organosorb 10-CO granular AC was provided by Desotec (Roeselare, Belgium).

2.2. Preparation of ACs derived from olive cake

Olive cake composed of olive pulp and olive stone was dried using an electrical oven at 120°C for 24 h.

Table 1
Egyptian production of olive oils & table olive between 1990 and 2012 (in 1,000 tones)

	90/91	95/96	2000/1	2005/6	2009/10	2011/12
Olive oils	0.5	2.5	0.5	2.5	3.0	5.0
Table olive	10.5	60.0	70.0	200.0	409.0	500.0

Subsequently, the dried sample was ground and sieved into a fraction between 500 and 850 μm. This fraction was used for the production of two types of ACs by chemical activation after impregnation with H_3PO_4 followed by pyrolysis for 2 h. The first (AC1) was impregnated with H_3PO_4 (60%) at ratio of 1:1.75 (w/w, olive cake: H_3PO_4) followed by pyrolysis at 450˚C for 2 h under nitrogen flow [21]. The second (AC2) was soaked with phosphoric acid (85 wt. %) at ratio of 1:3 (w/w, olive cake: H_3PO_4), the impregnated solid was activated into furnace tube and the temperature was raised to 500˚C for 2 h at a rate of 5˚C min^{-1} under forced air. The acid was removed by washing with distilled water till the pH reached 6.8. The carbon product was dried at 110˚C for 24 h using an electric oven. Commercial Organosorb 10-CO was used as a reference adsorbent.

2.3. Characterization of biomass and sorbent agents

Physicochemical properties were investigated by several techniques; elemental analyses were conducted with a CHNS elemental analyzer (Thermo Electron Flash EA 1112). The porous structure parameters were determined from nitrogen adsorption isotherms measured at 77 K with NOVA 2200 Gas Sorption Analyzer (Quantachrome). Prior to the measurements, the sample was outgassed overnight at 300˚C. The specific surface area (S_{BET}) was estimated by Brunauer–Emmett–Teller (BET) equation. The amount of nitrogen adsorbed at the relatively pressure of $p/p_0 = 0.96$ was employed to determine the total pore volume (V_T). The micropore volume ($V_{D–R}$) was calculated by applying the Dubinin–Radushkevich (D–R) equation. The mesopore volume (V_{mes}) was calculated as a difference between V_T and $V_{D–R}$. The pore size distributions (PSDs) were determined by means of the quenched solid density functional theory.

The surface topography of the ACs, the texture, and the pore structure was carried out using scanning electron microscope (SEM). For identification and distribution of elemental composition on the surface of ACs, energy dispersive X-ray analysis (EDX) was applied in combination with SEM analysis. SEM–EDX is performed with a FEI Quanta 200 FEG-SEM equipped with a Bruker Si(Li) EDX detector.

2.4. Determination of lead ions concentration

At the end of each experiment, the solution was filtered using a Whatman No. 42 filter paper and the lead concentrations were determined using ICP-AES. ICP-AES analysis is carried out using a PerkinElmer Optima 3300 DV ICP-AES spectrometer after calibration with a series of Pb calibration solutions. Linearity is guaranteed for a calibration range of 0.1–100 mg l^{-1}. All experiments were carried out in triplicate. Relative standard deviations were less than 5% in all experiments. The recovery was within the accepted range between 97 and 103%.

2.5. Preparation of tablets from AC as a final or semifinal product

Organosorb 10-CO and polytetrafluoroethylene was mixed in 10:1 ratio, respectively. Few drops of NMP (N-methyl-2-pyrrolidone) were added to the above mixture to form a homogeneous mixture. Obtained mixture was compressed using press machine to form a tablet. Tablets were heated at 100˚C under vacuum for 1 h to evaporate the rest solvent (NMP). The dried tablets were used as a primary study for Pb (II) ions uptake from aqueous solution at initial levels of 20 and 40 mg l^{-1}.

2.6. Batch sorption experiments

To avoid pH effects on lead ions precipitation, 20 mg l^{-1} of lead solution was run without sorbent agent at pH values of 2, 3, 4, 5, 5.5, 6, and 7 for 60 min at room temperature (25˚C) and 120 rpm using thermostatic shaker. To specify the optimum pH value for the adsorption capacity of the different adsorbent agents, 100 ml of lead solution with initial concentration of 20 mg l^{-1} was incubated with each sorbent (0.1 g) at different pH values of 2, 3, 4, 5, 5.5, 6, 6.5, and 7. The pH was adjusted using a NaOH solution (1, 0.1, 0.01 M) or a HCl solution (0.1, 0.1, 0.01 N) and measured electrochemically (pH-meter 764 Multi-Calimatic).

To study lead sorption kinetics of ACs and Organosorb 10-CO, a set of 100 ml of lead solutions with concentration level of 20 mg l^{-1} were incubated each with 0.1 g of sorbent agent. The mixtures were agitated at 120 rpm using thermostatic shaker at 25˚C for 5, 10, 20, 30, 40, 50, 60, 90, 120, 180, and 240 min.

The samples were filtered using Whatman filter paper No. 42 before ICP-AES measurements. The equilibrium time for each sample was fixed when no further decrease in lead ion concentration occurred.

The effect of carbon dose (CD) was carried out using 100 ml of lead solution with initial level of 40 mg l^{-1} The solutions were incubated with different CD (0.1, 0.15, 0.20, 0.30, and 0.40 g) and the mixtures were agitated at 120 rpm using thermostatic shaker at 25℃ till equilibrium time for each sorbent.

Different initial concentrations of Pb (II) ions (20–200 mg l^{-1}) were run to study the ability and maximal adsorption capacity for both ACs and the reference carbon.

The removal efficiency (%R), equilibrium time (q_t), and uptake (q_e) of adsorbent were calculated according to the following equations:

$$\%R = [(C_0 - C_e)/C_0] \times 100 \tag{1}$$

$$q_e \text{ or } q_t = (C_0 - C_e)V/m \tag{2}$$

where C_0 and C_e are the initial and equilibrium concentration of lead ions (mg l^{-1}), V is the volume of solute solution (l), and m is the weight of the adsorbent used (g).

3. Results and discussion

3.1. Characterization of sorbent agents

3.1.1. Elemental composition of the sorbent agents

The results of elemental analyses for olive cake, ACs, and Organosorb CO-10 are presented in Table 2.

The results showed that the carbon content of olive cake (56%) was higher than most of agricultural by-products (44%) [22]. This is due to the enhanced concentration of lignin which consists of three-dimensional networks of phenyl propane units, linked by C–C and C–O–C bonds, making its elemental composition higher in carbon content (62%) [23]. AC1 had a relatively high percent of carbon content (75%) than AC2 (72%); however, commercial Organosorb 10-CO had the highest percent of carbon content (83%). Pyrolysis of olive cake leads to carbon gasification which raises the ash content from 6.3% for biomass to 7.73% for AC2 and decreased to 4.64% for AC1.

3.1.2. Analysis of porous texture

The specific surface area, texture porosity, and PSD of ACs and Organosorb 10-CO are presented in Table 3 and Figs. 1 and 2. Referring to Table 3, it is clear that Organosorb 10-CO had the highest specific surface area followed by AC2 and AC1. PSD, a very important property of adsorbents, which determines the fraction of the total pore volume accessible to molecules of a given size and shape. The PSD (according to the IUPAC classification) of Organosorb 10-CO (Fig. 2) showed that a vast majority of the pores fall into the range of micropore ($d < 2$ nm). However, the total pore volume (V_T) reached 0.676 $cm^3 g^{-1}$ for AC2; AC1 and Organosorb 10-CO had almost similar V_T (0.448 and 0.432 $cm^3 g^{-1}$, respectively). Regarding the mesopore volume (V_{mes}) for AC2, a 2.5 and 50 times greater compared with AC1 and Organosorb 10-CO, respectively. This is due to the high concentration of H_3PO_4 used for impregnation, the main development corresponding to mesoporosity, which reached values higher than the $V_{D\text{–}R}$ [24].

The micropore volume ($V_{D\text{–}R}$) constituted 69% of V_T for AC1 and 47.5% for AC2. However, V_{mes} increased and reached 52.5% of V_T for AC2 compared to 31% for AC1. The increasing of micropore volume for AC1 could be explained due to the rapid development of microporosity at low concentration of phosphoric acid, since there is a relation between porosity and impregnation ratio. Organosorb 10-CO consists almost purely out of micropore volumes, therefore no hysteresis was found in their N_2 adsorption–desorption isotherm.

Table 2
Elemental analyses for biomass, ACs derived from olive cake and Organosorb 10-CO

	Elemental contents (%)				
Sorbent agents	C	N	H	S	O
Olive cake	55.86 ± 0.85	1.50 ± 0.10	7.44 ± 0.14	BDL	35.38 ± 0.84
AC1	74.79 ± 1.54	0.58 ± 0.01	3.18 ± 0.10	BDL	21.44 ± 0.61
AC2	71.58 ± 1.32	0.46 ± 0.01	4.54 ± 0.13	BDL	23.42 ± 0.73
Organosorb 10-CO	83.46 ± 1.84	0.41 ± 0.02	0.498 ± 0.01	0.956 ± 0.06	14.67 ± 0.39

Notes: AC1—AC derived from olive cake under N_2; AC2—AC derived from olive cake under air; Organosorb 10-CO—a reference carbon; O—oxygen percent on ash free basis; and BDL—below detection limit (0.03 mg).

Table 3
Porous texture parameters determined by nitrogen sorption at 77 K

Activated carbon	S_{BET} ($m^2 g^{-1}$)	V_T ($cm^3 g^{-1}$)	$V_{D\text{–}R}$ ($cm^3 g^{-1}$)	V_{mes} ($cm^3 g^{-1}$)	$V_{D\text{–}R}/V_T$ (%)	V_{mes}/V_T (%)
AC1	793	0.448	0.310	0.138	69.2	30.8
AC2	835	0.676	0.321	0.355	47.5	52.5
Organosorb 10-CO	1,000	0.432	0.425	0.007	98.4	1.6

Notes: $^{V}{}_{T}$—total pore volume; $V_{D\text{–}R}$—micropore volume; and V_{mes}—mesopore volume.

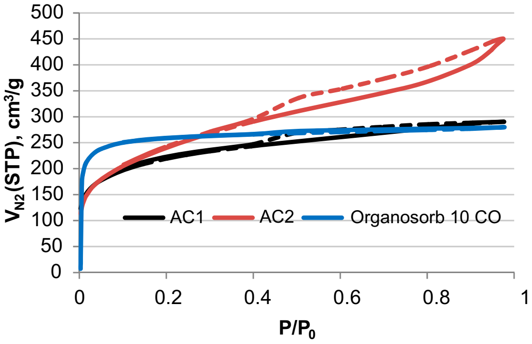

Fig. 1. N_2 sorption adsorption–desorption isotherms measured at 77 K.

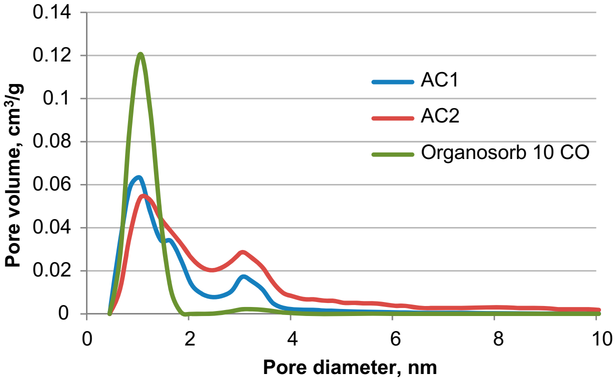

Fig. 2. PSD of ACs and Organosorb 10-CO.

The effect of air atmosphere leads to enhanced gasification of carbon associated with generation of O-functionalities imparting surface acidity [10].

It is well known that the surface of AC should be hydrophobic with very low affinity for water adsorption [25]. The presence of heteroatoms, especially oxygen, available as active chemical groups analogous to organic species, become primary adsorption centers, due to their polarity and possibility to attract water via hydrogen bonding [26].

3.1.3. SEM photographs

The SEM images reflect the efficiency of thermochemical activation by phosphoric acid in increasing the porosity of both ACs treated under N_2 and forced air. Referring to Fig. 3, the produced ACs have external surface with full cavities compared to Organosorb 10-CO. Also, the pores were different in size and in shape.

It is evident from Fig. 3 that the morphology of the carbon (AC1, Fig. 3(a)) impregnated with low H_3PO_4 impregnation ratio (1:1.75; precursor: acid) is almost identical to that of the char, but increasing concentrations of the phosphoric acid impregnation as in AC2 (1:3; precursor: acid) showed a surface that is more clearly attacked (Fig. 3(b)). The original cellular morphology of the precursor is lost because a large part of the cellulosic structure has been degraded and extracted from the interior to the exterior of the particle [27]. Referring to Fig. 3(c), the observed white spots can be assigned to lead adsorption on the surface of AC after lead adsorption experiment, which is also confirmed by the EDX spectrum (Fig. 4(d)).

The EDX analysis (Fig. 4(a), (c), and (d)) showed that treatment of olive cakes with high concentration of phosphoric acid enhanced the acid interactions with lignocellulosic materials and phosphorylation of cellulose [28]. This leads to formation of phosphate esters and promotes cross-linking reactions and pore development. The observed sodium content in AC2 after lead adsorption (Fig. 4(d)) is the result of NaOH treatment used for solution pH adjustment which led to the conversion of the acid groups into their sodium salt form [29]. The observed contents of silicon and calcium for AC1 and AC2 are due to the natural occurrence in the carbonaceous raw materials. For Organosorb 10-CO, besides a high percent of carbon, also sulfur, silicon and potassium were found in small amounts (Fig. 4(b)). Referring to Fig. 4(d), the observed lead content in AC2 referred to lead adsorption on the surface of AC after lead adsorption experiment.

3.2. Adsorption experiments

3.2.1. Effect of initial pH values

The pH of metal solutions has been identified as the major parameter controlling metal sorption

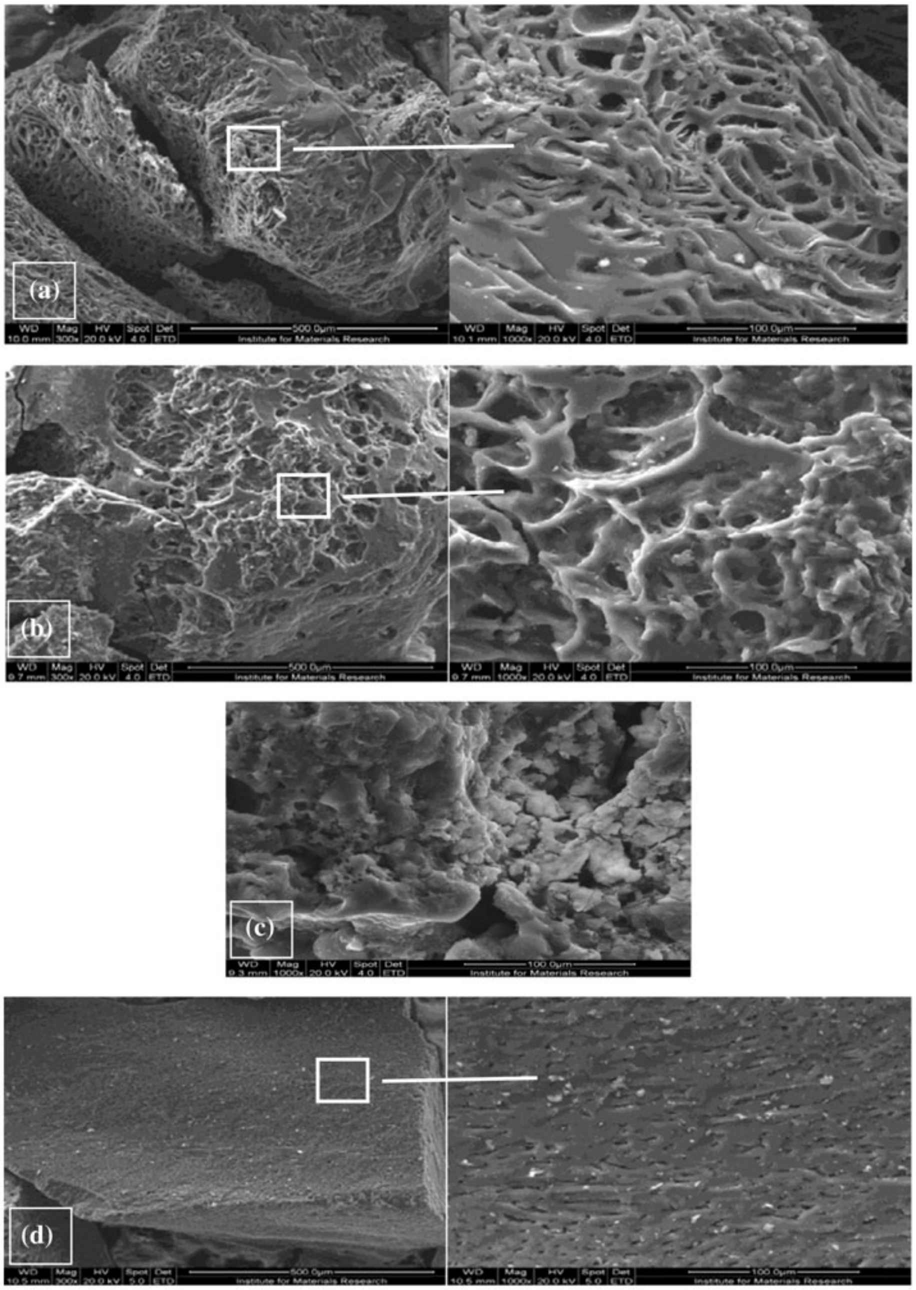

Fig. 3. SEM images for (a) AC1, (b) AC2, (c) AC2 after lead adsorption, and (d) Organosorb 10-CO at magnification of 300× and 1000×.

processes [30]. This is partly due to the fact that protons are strong competing sorbates, and partly to the fact that the solution pH influences the ionization of functional groups of the sorbate and the chemical speciation of lead ions in solution.

To distinguish between lead ion adsorption and lead ion precipitation, the result in Fig. 5 stated that, with increasing pH values, the precipitation of lead ions at a level of 20 mg l^{-1} increased gradually from 49 at pH 6 to 58% at pH 6.5 and was nearly completed at pH 7. However, there was no observed precipitation of lead ions at pH value of 5.5. The same trend was found by Ibrahim et al. [31] who found that at initial concentration of Pb (II) of 50 mg l^{-1}, the percentage of lead removal by precipitation was 35% at pH 6.5, however it reached 76% at pH 7.5. Referring to Fig. 6, no adsorption for AC1 and Organosorb 10-CO at pH 2 and 3 was observed. However, 21 and

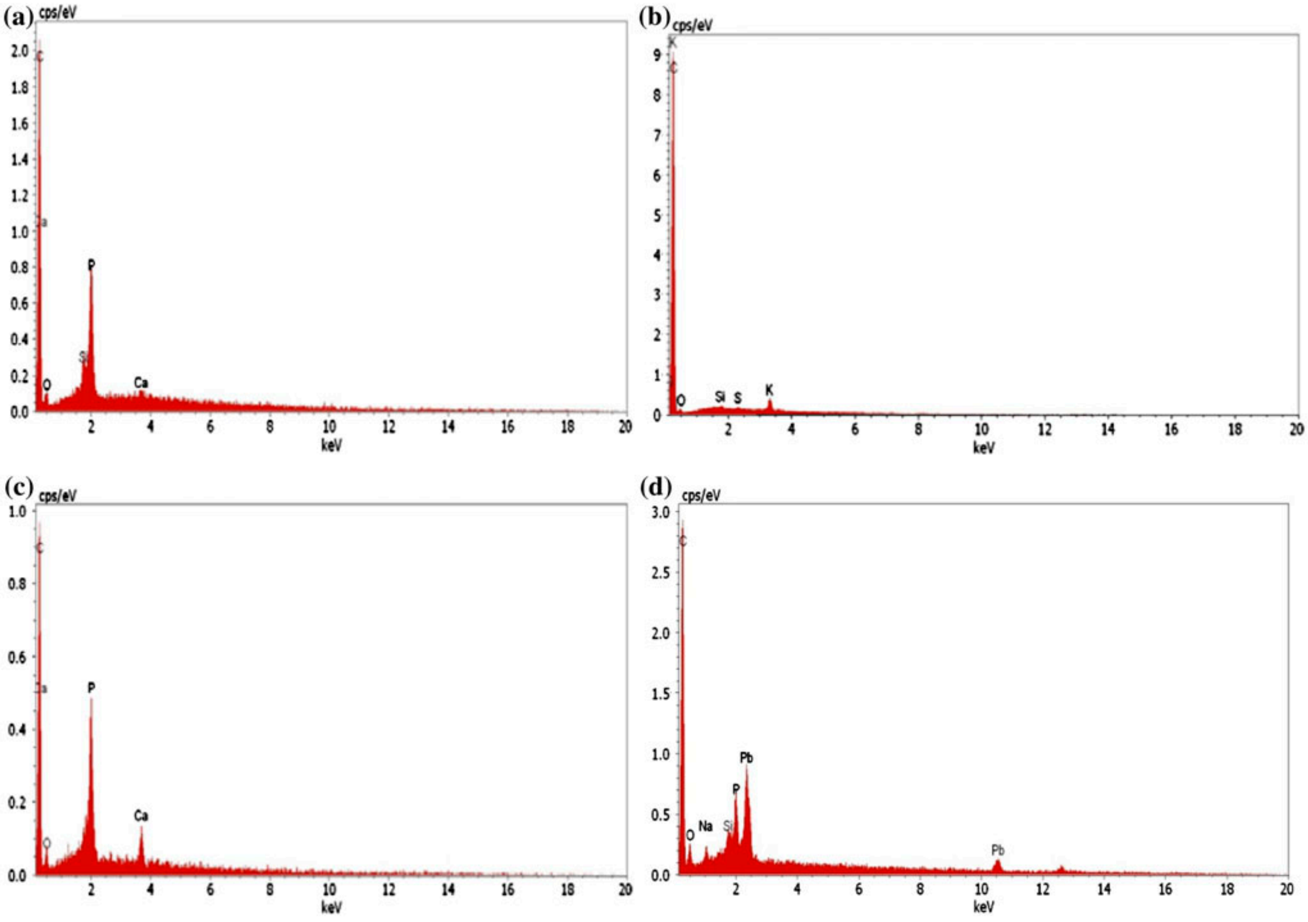

Fig. 4. EDX spectrum of (a) AC1, (b) Organosorb 10-CO, (c) AC2, and (d) AC2 after lead adsorption.

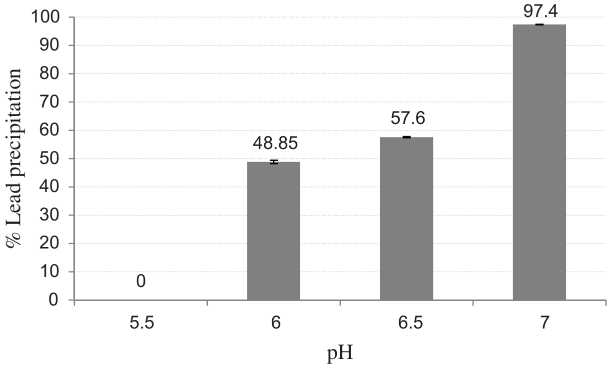

Fig. 5. Effect of pH on lead ion precipitation at a level of 20 mg l^{-1} (T, 25 ± 1 ℃).

46% removal for AC2 at the same pH values were obtained. From Fig. 6 one can be concluded that the removal percentage of lead ions increases as pH increases.

This trend can be explained by the competitive effect. At low pH values, the hydrogen ions will be increased and predominant. So, the H^+ and Pb (II) ions compete for the negative adsorption sites on the carbon surface. With the increasing of pH values, the

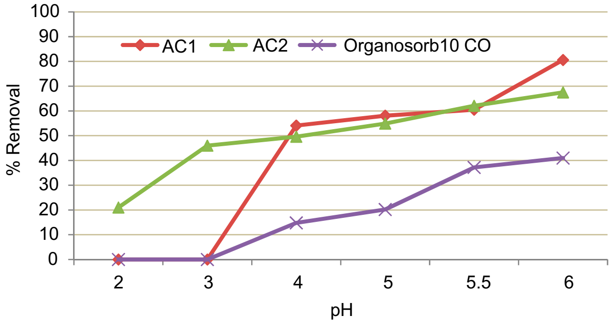

Fig. 6. Effect of pH on the adsorption capacity of ACs and Organosorb 10-CO. Experimental conditions (0.1 g adsorbent, 20 mg l^{-1} of lead ions, and $T = 25 \pm 1$ ℃).

adsorption of Pb (II) ions was increased due to the decrease in the concentrations of H^+ ions and thus will not have the opportunity to compete with Pb (II) ions on the adsorption sites [32]. Also, the surface of ACs become more negatively charged which attracts the positive charge of Pb (II) ions [33]. This finding is supported by Gurgel and Gil and Lui et al. [34,35] who stated that at low pH values, the electrostatic interaction between Pb (II) and protonated surfaces of ACs becomes very poor since at lower pHs, most acidic groups were in protonated forms. So, the uptake of Pb (II) was difficult as a result of the less electrostatic attraction.

Taking into account, the results obtained in Fig. 5 a pH value of 5.5 was chosen as the optimum pH for studying solely the Pb adsorption.

3.2.2. Effect of contact time

Data presented in Fig. 7 showed sorption kinetics of each sorbent against Pb (II) ions (20 mg l^{-1} of lead solution, 0.1 g adsorbent, 25˚C, and pH 5.5). The results indicated that 45 and 48% of lead ions were adsorbed within 30 min onto AC1 and AC2, respectively, in contrast to a limited uptake of lead for Organosorb 10-CO (27% after 30 min). It is evident from Fig. 7 that maximal adsorption was achieved within 2 h (76 and 81% for AC1 and AC2, respectively). About 3 h was required to reach the maximum lead removal for Organosorb 10-CO of only 59%.

The aforementioned results suggested that at the initial stage of the contact, the adsorption of the Pb (II) ions onto the ACs occurred rapidly, followed by a second more slowly adsorption stage. In a third stage, the adsorption reached equilibrium where the amount of Pb (II) ions being adsorbed onto the AC was equal to the amount of Pb (II) desorbing from the AC. The rapid adsorption at the initial adsorption is mainly due to the availability of a larger number of vacant surface sites [36,37].

3.2.3. Effect of tablet form of commercial AC

The tablet Organosorb 10-CO produced from regular commercial AC was tested as a function of time for the adsorption of Pb (II) ions. As shown in Fig. 8, the results indicated that more time (48 h) is required to achieve the equilibrium time than the granular Organosorb 10-CO. On the other hand, at initial level of 20 mg l^{-1} of Pb (II) ions, the granular Organosorb 10-CO was able to remove 59% of Pb (II) ions while only 16.4% of Pb (II) ions were removed within 3 h for the tablet form. At high initial concentration of Pb (II) ions level (40 mg l^{-1}), a decrease in the lead removal percentage is found. Indeed, after 24 h, the percentage of removal reached 76 and 50% for the tablet AC at initial lead levels of 20 and 40 mg l^{-1}, respectively. However, 48 h are needed to remove 84 and 62% of Pb (II) ions for tablet AC at initial levels of 20 and 40 mg l^{-1}, respectively. This results indicated that 48 h is not enough to reach the equilibrium state for the tablet form derived from Organosorb 10-CO for lead ions at initial concentration levels of 20 and 40 mg l^{-1}.

3.2.4. Effect of CD

The removal efficiency and Pb (II) ions adsorption as a function of CD are presented in Fig. 9. It is noticed that with increasing CD, the removal percentage of Pb (II) ions goes through a minimum at 1.5 g l^{-1} AC1 and AC2 up to a maximum value at 2 g l^{-1}. Then removal percentage of Pb (II) ions decreased as CD further increased up to 4 g l^{-1}. As can been seen from Fig. 9, the amount of adsorbed lead continuously increased as a function of the CD,

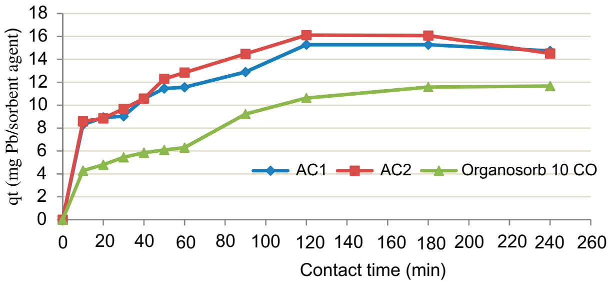

Fig. 7. Effect of contact time on the adsorption capacity of ACs against lead(II) ions. Experimental conditions (0.1 g adsorbent, 20 mg l^{-1} of lead ions, 100 ml solution, pH 5.5, and $T = 25$˚C).

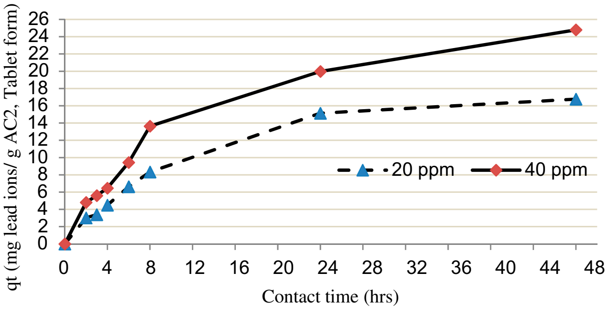

Fig. 8. Effect of contact time on the adsorption capacity of Organosorb 10-CO tablet for lead ions. Experimental conditions (0.1 g tablet Organosorb 10-CO, pH 5.5, and $T = 25 \pm 1$˚C).

but is not reflected in a higher lead removal percentage. Rather a constant lead removal percentage is found for AC1 and AC2. For Organosorb 10-CO, a different pattern is found: the lead removal percentage clearly increased as a function of the increasing CD, despite the fact that the amount of adsorbed lead systematic increased.

Although the surface area of commercial AC (Organosorb 10-CO) was the highest among the tested ACs, the adsorption capacity was the lowest. The surface area is clearly not the only key parameter for lead adsorption. Also the kind of pores in combination with the presence of organic functional groups play an important role, clearly demonstrated in this case. Organosorb 10-CO has only micropores, AC1 and AC2 have micro- and mesopores. AC1 and AC2 have also a much higher oxygen content related to more oxygen containing organic functional groups, acting as complexing agents toward the Pb (II) ions to be bound on the AC surface. Finally, an adsorbate molecule does not simply enter into the pores and stay there, it will, on average, move in and out about 10^{15} times per second. At equilibrium, the number of molecules entering the pores equals the number of molecules leaving. This concept of mobility and exchange is based on isotopic exchange studies. In addition, it is important to note that the adsorption sites of AC are different from each other by having its own potential energy. Moreover, not all of the pores of an AC have the same entrance dimensions [38].

3.3. Adsorption isotherms

The Langmuir and Freundlich models are the most frequently employed to describe experimental data of adsorption isotherms. In the current work, both models were used to describe the relationship between the amount of Pb (II) ions adsorbed and its equilibrium concentration in solution and compared with the Dubinin–Kaganer–Radushkevich (D–K–R) isotherm.

3.3.1. Langmuir isotherm

Langmuir isotherm presupposes mono layer adsorption onto a surface containing a finite number of adsorption sites via uniform strategies of adsorption. The linear form of Langmuir isotherm model [39] is described by the following equation:

$$C_e/q = 1/q_{\max} \cdot K_L + C_e/q_{\max} \tag{3}$$

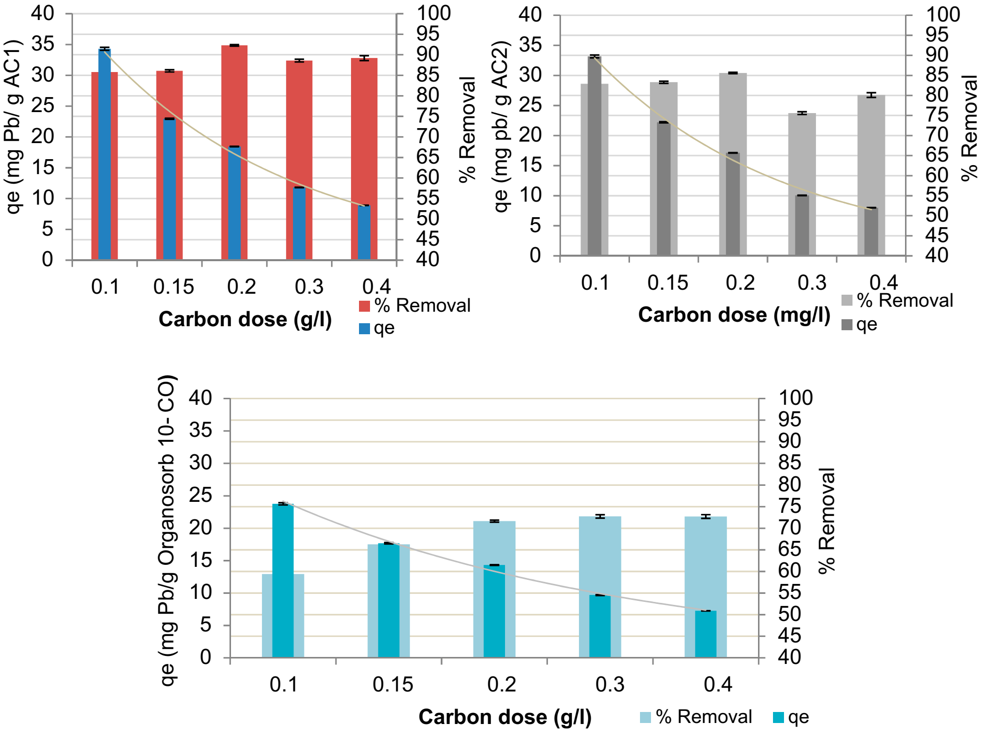

Fig. 9. Effect of CD on the adsorption capacity of sorbent agents (a) AC1, (b) AC2, and (c) granular Organosorb 10-CO for lead (40 mg l^{-1} of lead, pH 5.5, $T = 25 \pm 1$°C, and q_t for each sorbent).

where C_e (mg l^{-1}) is the concentration of metal in solution at equilibrium, q (mg g^{-1}) is the amount of metal sorbed per unit mass of AC, $q_{\max}$ the maximum adsorption capacity (mg g^{-1}), and K_L (l mg^{-1}) are Langmuir constants related to mono layer capacity sorption and sorption energy, respectively.

3.3.2. Freundlich isotherm

The Freundlich isotherm, on the other hand, assumes a heterogeneous surface energy in which the energy terms varies as a function of surface coverages. The Freundlich isotherm (Eq. (4)), usually fits the experimental data over a wide range of concentrations. This isotherm gives an expression encompassing the surface heterogeneity and the exponential distribution of active sites and their energies. It describes the equilibrium on heterogeneous surfaces and does not assume monolayer capacity [40,41] and is given by the following equation:

$$\log q_e = \log K_f + 1/n \log C_e \tag{4}$$

K_f and n are the Freundlich constants related to the adsorption capacity and the intensity or heterogeneity of adsorption.

3.3.3. D–K–R isotherm

Freundlich and Langmuir isotherms could not provide any information about the sorption mechanism. The D–K–R isotherm is an analog of Langmuir type, but it is more general because it does not assume a homogeneous surface or constant sorption potential [42]. The D–K–R isotherm model was used to predict the nature of adsorption processes as physical or chemical [43].

The linearized D–K–R isotherm equation can be written as:

$$\ln q_e = \ln X_m - \beta\varepsilon^2 \tag{5}$$

where q_e is the number of metal ions adsorbed per unit weight of adsorbent (mol g^{-1}), X_m is the maximum sorption capacity, β is the activity coefficient related to mean sorption energy, and ε is the Polanyi potential, which is equal to:

$$\varepsilon = RT \ln\left(1 + \frac{1}{C_e}\right) \tag{6}$$

where R is the gas constant (J mol^{-1} K) and T is the temperature (K). The saturation limit X_m may represent the total specific micropore volume of the sorbent. The sorption potential is independent of the temperature but varies according to the nature of sorbent and sorbate [44]. The sorption space in the vicinity of a solid surface is characterized by a series of equipotential surfaces having the same sorption potential. The sorption energy can also be calculated using the following equation:

$$E = 1/(-2\beta)^{1/2} \tag{7}$$

3.3.4. Langmuir isotherm

A linear plot was obtained when C_e/q is plotted against C_e over the concentration range of Pb concentrations investigated (Fig. 10). The Langmuir model effectively and significantly described the sorption data for AC1 and Organosorb 10-CO with R^2 values 0.9839 and 0.9767, respectively. On the other hand, sorption of Pb onto AC2 is poorly fitted using Langmuir isotherm ($R^2 = 0.8579$). According to the $q_{\max}$ (mg g^{-1}) parameter in Table 4, mono layer capacities of ACs are arranged in the following sequence, AC2 > AC1 > Organosorb 10-CO.

Pb seems to reach saturation, which means that Pb had closed possible available sites in ACs and further adsorption could take place only at new surfaces.

Adsorption capacities of Pb with AC types listed in Table 4 were 58.14, 39.8, and 188.67 mg g^{-1} for AC1, Organosorb 10-CO, and AC2, respectively. Their results indicated the following sequence: AC2 > AC1 > Organosorb 10-CO, as confirmed by Fig. 10. The higher adsorption capacities observed for AC1 and AC2 compared to Organosorb 10-CO could be related

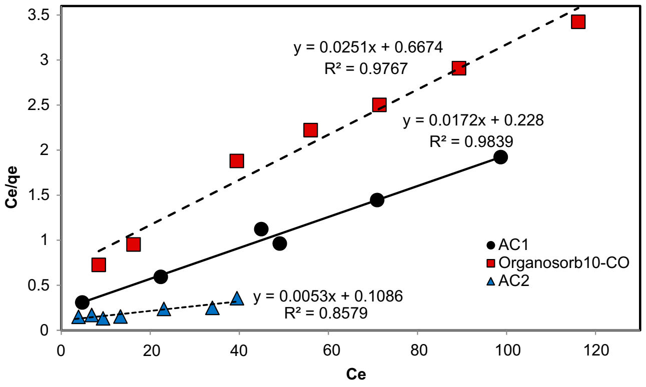

Fig. 10. Langmuir isotherm model for the adsorption of Pb on ACs. Experimental conditions (0.1 g adsorbent, different initial concentration of lead ions, 100 ml solution, pH 5.5, and $T = 25 \pm 1$°C).

Table 4
Langmuir equation constants of Pb uptake by ACs

	AC1	Organosorb 10-CO	AC2
$q_{\max}$ (mg g^{-1})	58.14	39.8	188.67
K_L (l mg^{-1})	0.075	0.0376	0.0488
R_L	0.4	0.57	0.51
R^2	0.9839	0.9767	0.8579

Notes: R^2—correlation coefficient. Experimental conditions: (0.1 g of adsorbent; 20–200 mg l^{-1} of Pb (II); pH = 5.5; and $T = 25 \pm 1$℃).

to the porosity and adsorption sites available on these ACs. The high mesopore volume for AC2 and AC1 (0.355 and 0.138) than Organosorb 10-CO as in Table 3 may explain the high adsorption capacity for AC1 and AC2. The separation factor R_L (dimensionless constant) which is the essential characteristic of Langmuir model can be calculated from the following equation [45]:

$$R_L = 1/(1 + K_L C_0) \tag{8}$$

where C_0 is the initial concentration of adsorbate (mg l^{-1}) and K_L (l mg^{-1}) is Langmuir constant. The value of R_L indicates the shape of the isotherm to be either unfavorable ($R_L > 1$), linear ($R_L = 1$), favorable ($0 < R_L < 1$), or irreversible ($R_L = 0$) [46]. The R_L values between 0 and 1 indicate favorable adsorption. The value of R_L for the adsorption of Pb on ACs was 0.4, 0.57, and 0.51 for AC1, Organosorb 10-CO, and AC2, respectively (Table 4), and thus a favorable process.

These results indicated that the adsorption of Pb on the surface of studied ACs was a favorable process.

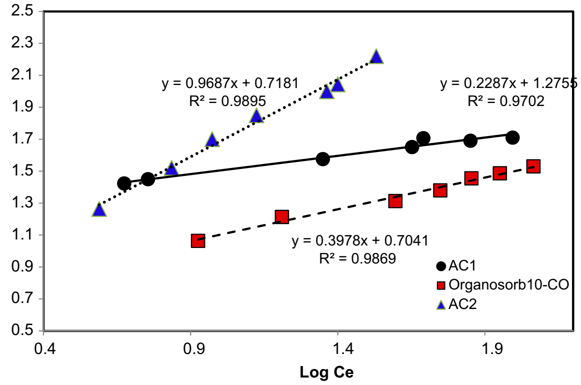

Fig. 11. Freundlich isotherm model for the adsorption of Pb on ACs.

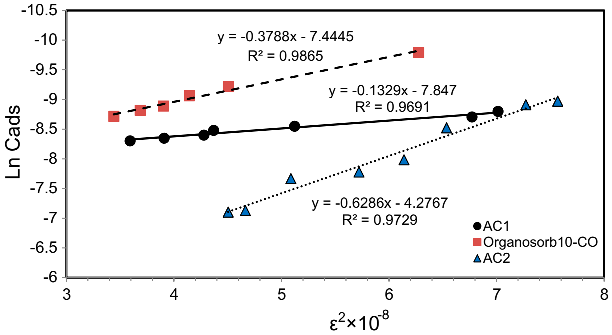

Fig. 12. D–K–R isotherm model for the adsorption of Pb on ACs.

3.3.5. Freundlich isotherm

The Freundlich isotherms were also applied to the removal of Pb using the ACs under study. Referring to Tables 4 and 5, adsorption seems to fit the Freundlich isotherm as well as the Langmuir isotherm [47]. However for AC2, there is a clear preference for the Freundlich isotherm. The constants K_f and n are calculated for each ACs as shown in Table 5.

A linear plot is obtained when log C_e is plotted against log q_e over the entire concentration range of Pb investigated with R^2 values of 0.9702, 0.9869, and 0.9895 for ACs AC1, Organosorb 10-CO, and AC2, respectively (Fig. 11).

$1/n$ values for ACs AC1, Organosorb 10-CO, and AC2 were 0.2287, 0.397, and 0.9687 which reveals that n are 4.37, 2.518, and 1.032 for ACs AC1, Organosorb 10-CO, and AC2, respectively. As shown in Table 5,

Table 5
Freundlich adsorption constants for Pb uptake by ACs at 25 ± 1℃

K_f			n			R^2		
AC1	O 10-CO	AC2	AC1	O10-CO	AC2	AC1	O10-CO	AC2
18.858	5.059	5.225	4.37	2.514	1.032	0.9702	0.9869	0.9895

Notes: R^2—correlation coefficient; O 10-CO—Organosorb 10-CO. Experimental conditions: (0.1 g of adsorbent; 20–200 mg l^{-1} of Pb (II); pH = 5.5; and $T = 25 \pm 1$℃).

Table 6
D–K–R equation constants of Pb uptake by ACs

	AC1	Organosorb 10-CO	AC2
X_m (mol g^{-1})	0.000908	0.000585	0.0139
β (mol^2 J^{-2})	-0.1329×10^{-8}	-0.3788×10^{-8}	-0.6286×10^{-8}
Energy (kJ mol^{-1})	19.37	11.49	8.92
R^2	0.9691	0.9865	0.9729

Notes: R^2—correlation coefficient. Experimental conditions: (0.1 g of adsorbent; 20–200 mg l^{-1} of Pb (II); pH = 5.5; and $T = 25 \pm 1$°C).

good adsorption for ACs AC2 and Organosorb 10-CO are obtained than for AC1 because $1/n$ value of AC1 is lower than for AC2 and much lower than for Organosorb 10-CO.

The results show that the value of n is greater than unity for ACs indicating that the Pb is favorably adsorbed by the ACs [48,49]. This is in agreement with the findings regarding to R_L values of Langmuir equation. The magnitude of Freundlich constant indicates easy uptake of Pb from aqueous solution by AC2 and Organosorb 10-CO than AC1.

3.3.6. D–K–R isotherms

Fig. 12 represented the D–K–R plot of the adsorption of Pb (II) ions onto ACs AC1, Organosorb 10-CO, and AC2.

The mean energy of adsorption "E" gives information about the adsorption mechanism, physical or chemical. If E value < 20 kJ mol^{-1}, the adsorption process takes place physically [50], which is the case here (Table 6).

The mean sorption energy was calculated as 19.36, 11.48, and 8.92 kJ mol^{-1} for the adsorption of Pb (II) ions on AC1, Organosorb 10-CO, and AC2, respectively (Table 6).

4. Conclusion

The ACs derived from olive cake has considerable potential for the removal of Pb (II) ions from aqueous solution under different conditions and over a wide range of concentrations. Organosorb 10-CO as a reference carbon had a limited adsorption capacity in its granular form. The high mesoporosity of AC2 is mainly due to the high concentration of phosphoric acid used during the activation process, since it recorded 52.5 of total pore volume toward 31% for AC1. However for Organosorb 10-CO, the vast majority of the pores fall into the range of micropore volume. The total pore volume of AC2 (activated under forced air) recorded the highest one (0.676 cm^3 g^{-1}) followed by AC1 (0.448 cm^3 g^{-1}) and then Organosorb 10-CO (0.432 cm^3 g^{-1}). Although the surface area of Organosorb 10-CO as a reference carbon recorded 1,000 m^2 g^{-1} and was the highest among the tested ACs, however the adsorption capacity toward Pb (II) ions was the lowest. Batch adsorption kinetic experiments revealed that the maximum adsorption capacity ($q_{\max}$) was achieved within 2 h for AC1 and AC2; however, 3 h was required for Organosorb 10-CO. Langmuir isotherm provided a maximum adsorption capacity of 58.139, 188.67, and 39.84 mg g^{-1} for AC1, AC2, and Organosorb 10-CO, respectively. The sorption energy (E-value) was 19.36, 8.92, and 11.48 kJ mol^{-1} for the tested ACs, respectively, which indicated that the adsorption process takes place. The results clearly indicated that AC2 had the highest adsorption capacity toward Pb (II) ions. A final product of AC in tablet forms was achieved and succeeded in the removal of Pb (II) ions from aqueous media but it need much more time to reach equilibrium, but realizing higher Pb (II) ions removal percentage.

References

[1] J. García-Lestón, J. Méndez, E. Pásaro, B. Laffon, Genotoxic effects of lead: An updated review, Environ. Int. 36 (2010) 623–636.
[2] F.M. Johnson, The genetic effects of environmental lead, Mutat. Res. 410 (1998) 123–140.
[3] R.R. Jones, The continuing hazard of lead in drinking water, Lancet 2 (1989) 669–670.
[4] UNEP/UNICEF (United Nations Environment Programme/United Nations Children's Fund (UNICEF)), Childhood Lead Poisoning—Information for Advocacy and Action, 1997. Available from: <http://www.chem.unep.ch/irptc/Publications/leadpoison/lead_eng.pdf>.
[5] A. Balaria, S. Schiewer, Assessment of biosorption mechanism for Pb binding by citrus pectin, Sep. Purif. Technol. 63 (2008) 577–581.
[6] S. Bhattacharjee, S. Chakrabarty, S. Maity, Removal of lead from contaminated water bodies using sea nodule as an adsorbent, Water Res. 37 (2003) 3954–3954.
[7] L. Patrick, Lead toxicity, a review of the literature. Part 1: Exposure, evaluation, and treatment, Altern. Med. Rev. 11 (2006) 2–22.
[8] V.K. Gupta, A. Rastogi, Biosorption of lead from aqueous solutions by green algae *spirogyra* species: Kinetics and equilibrium studies, J. Hazard. Mater. 152 (2008) 407–414.

[9] A.A. El-Kady, H.A.S. Sharaf, Abbès, J. Ben Salah-Abbès, K.H. Naguib, R. Oueslati, M.A. Abdel-Wahhab, Adsorption of Cd^{2+} ions on an Egyptian montmorillonite and toxicological effects in rats, Appl. Clay Sci. 44 (2009) 59–66.

[10] B.S. Girgis, A.A. El-Kady, A.A. Attia, N.A. Fathy, M.A. Abdel-Wahhab, Impact of air convection on H_3PO_4-activated biomass for sequestration of Cu (II) and Cd (II) ions, Carbon Lett. 10 (2009) 114–122.

[11] S. Al-Asheh, F. Banat, N. Al-Hamed, Adsorption of pollutants from aqueous solutions using activated and non-activated oak shells: Parametric and fractional factorial design study, part 1, Adsorption 21 (2003) 177–188.

[12] M. Karniba, A. Kabbani, H. Holail, Z. Olam, Heavy metals removal using activated carbon, silica and silica activated carbon composite, Energy Procedia 50 (2014) 113–120.

[13] T. Bohli, A. Ouederni, N. Fiol, I. Villaescusa, Evaluation of an activated carbon from olive stones used as an adsorbent for heavy metal removal from aqueous phases, C.R. Chim. 18 (2015) 88–99.

[14] A. Afkhami, T. Madrakin, Z. Karimi, Effect of the impregnation of carbon with ethylenediaminetetraacetic acid on its adsorption capacity for the adsorption of several metals ions, J. Hazard. Mater. 150 (2008) 408–412.

[15] International Olive Council (IOC), Web site of International Olive Council, 2012. Available from: <http://www.internationaloliveoil.org/>.

[16] A. Roig, M.L. Cayuela, M.A. Sánchez-Monedero, An overview on olive mill wastes and their valorisation methods, Waste Manage. 26 (2006) 960–969.

[17] M.J. Paredes, E. Moreno, A. Ramos-Cormenzana, J. Martinez, Characteristics of soil after pollution with wastewaters from olive oil extraction plants, Chemosphere 16 (1987) 1557–1564.

[18] M. DellaGreca, P. Monaco, G. Pinto, A. Pollio, L. Previtera, F. Temussi, Phytotoxicity of low-molecular-weight phenols from olive mill wastewaters, Bull. Environ. Contam. Toxicol. 67 (2001) 352–359.

[19] G. Rana, M. Rinaldi, M. Introna, Volatilisation of substances alter spreading olive oil waste water on the soil in a Mediterranean environment, Agric. Ecosyst. Environ. 96 (2003) 49–58.

[20] A. El-Hamouz, H.S. Hilal, N. Nassar, Z. Mardawi, Solid olive waste in environmental cleanup: Oil recovery and carbon production for water purification, J. Environ. Manage. 84 (2007) 83–92.

[21] R. Baccar, J. Bouzid, M. Feki, A. Montiel, Preparation of activated carbon from Tunisian olive-waste cakes and its application for adsorption of heavy metal ions, J. Hazard. Mater. 162 (2009) 1522–1529.

[22] B. Jibril, O. Houache, R. Al-Maamari, B. Al-Rashidi, Effects of H_3PO_4 and KOH in carbonization of lignocellulosic material, J. Anal. Appl. Pyrolysis 83 (2008) 151–156.

[23] A. Demirbas, Agricultural based activated carbons for the removal of dyes from aqueous solutions: A review, J. Hazard. Mater. 167 (2009) 1–9.

[24] H. Marsh, F. Rodriguez-Reinoso, Activation processes (chemical), in: M. Harry, R. Francisco (Eds.), Activated Carbon, Elsevier, 2006, pp. 322–365.

[25] A.M. Puziy, O.I. Poddubnaya, Characterization of surface heterogeneity of carbon-composite adsorbents, Mater. Sci. Forum 308 (1999) 908–913.

[26] F. Adib, A. Bagreev, T.J. Bandosz, Effect of surface characteristics of wood-based activated carbons on adsorption of hydrogen sulfide, J. Colloid Interface Sci. 214 (1999) 407–415.

[27] H. Marsh, F. Rodriguez-Reinoso, Applicability of activated carbon, in: M. Harry, R. Francisco (Eds.), Activated Carbon, Elsevier, 2006, pp. 383–453.

[28] M. Olivares-Marín, C. Fernández-González, A. Macías-García, V. Gómez-Serrano, Thermal behaviour of lignocellulosic material in the presence of phosphoric acid. Influence of the acid content in the initial solution, Carbon 44 (2006) 2347–2350.

[29] A. Aziz, M.S. Ouali, E. Elandaloussi, L.C. Menorval, M. Lindheimer, Chemically modified olive stone: A low-cost sorbent for heavy metals and basic dyes removal from aqueous solutions, J. Hazard. Mater. 163 (2009) 441–447.

[30] D. Kratochvil, B. Volesky, Advances in the biosorption of heavy metals, Trends Biotechnol. 16 (1998) 291–300.

[31] H.S. Ibrahim, A.A. El-Kady, N.S. Ammar, L. Meesuk, P. Wathanakul, M.A. Abdel-Wahhab, Application of isotherm and kinetic models for the removal of lead ions from aqueous solutions, J. Environ. Eng. 139 (2013) 349–357.

[32] M. Momčilović, M. Purenović, A. Bojić, A. Zarubica, M. Ranđelović, Removal of lead (II) ions from aqueous solutions by adsorption onto pine cone activated carbon, Desalination 276 (2011) 53–59.

[33] Z.A. Al-Anber, M.A.D. Matouq, Batch adsorption of cadmium ions from aqueous solution by means of olive cake, J. Hazard. Mater. 151 (2008) 194–201.

[34] L.V.A. Gurgel, L.F. Gil, Adsorption of Cu(II), Cd(II) and Pb(II) from aqueous single metal solutions by succinylated twice-mercerized sugarcane bagasse functionalized with triethylenetetramine, Water Res. 43 (2009) 4479–4488.

[35] H. Liu, P. Dai, J. Zhang, C. Zhang, N. Bao, C. Cheng, L. Ren, Preparation and evaluation of activated carbons from lotus stalk with trimethyl phosphate and tributyl phosphate activation for lead removal, Chem. Eng. J. 228 (2013) 425–434.

[36] B.H. Hameed, Equilibrium and kinetics studies of 2,4,6-trichlorophenol adsorption onto activated clay, Colloid Surf., A 1–3 (2007) 45–52.

[37] S.G. Poulopoulos, M. Nikolaki, D. Karampetsos, C.J. Philippopoulos, Photochemical treatment of 2-chlorophenol aqueous solutions using ultraviolet radiation, hydrogen peroxide and photo-Fenton reaction, J. Hazard. Mater. 153 (2008) 582–587.

[38] H. Marsh, F. Rodriguez-Reinoso, Characterization of activated carbon, in: M. Harry, R. Francisco (Eds.), Activated Carbon, Elsevier, 2006, pp. 143–242.

[39] I. Langmuir, Adsorption of gases on plain surfaces of glass mica platinum, J. Am. Chem. Soc. 40 (1918) 1361–1403.

[40] M. Prasad, H.-Y. Xu, S. Saxena, Multi-component sorption of Pb(II), Cu(II) and Zn(II) onto low-cost mineral adsorbent, J. Hazard. Mater. 154 (2008) 221–229.

[41] H. Freundlich, Adsorption in solution, Z Phys. Chem. 57 (1906) 384–470.

[42] A. Kilislioðlu, B. Bilgin, Thermodynamic and kinetic investigations of uranium adsorption on amberlite IR-118H resin, Appl. Radiat. Isot. 58 (2003) 155–160.

[43] M.M. Dubinin, E.D. Zaverina, L.V. Radushkevich, Sorption and structure of active carbons. I. Adsorption of organic vapors, Zhurnal Fizicheskoi Khimii 21 (1947) 1351–1362.

[44] S.A. Khan, U.R. Rehman, M.A. Khan, Adsorption of chromium (III), chromium (VI) and silver (I) on bentonite, Waste Manage. 15 (1995) 271–282.

[45] K.R. Hall, L.C. Eagleton, A. Acrivos, T. Vermeulen, Pore-and solid-diffusion kinetics in fixed-bed adsorption under constant-pattern conditions, Ind. Eng. Chem. Fundam. 5 (1966) 212–223.

[46] B.H. Hameed, J.M. Salman, A.L. Ahmad, Adsorption isotherm and kinetic modeling of 2,4-D pesticide on activated carbon derived from date stones, J. Hazard. Mater. 163 (2009) 121–126.

[47] S.M. Hasany, M.M. Saeed, M. Ahmed, Sorption and thermodynamic behavior of zinc (II)-thiocyanate complexes onto polyurethane foam from acidic solutions, J. Radioanal. Nucl. Chem. 252 (2002) 477–484.

[48] R.E. Treybal, Mass-transfer Operations, second ed., McGraw Hill, New York, NY, 1968.

[49] Y. Ho, G. McKay, Sorption of dye from aqueous solution by peat, Chem. Eng. J. 70 (1998) 115–124.

[50] W. Rieman, H. Walton, Ion Exchange in Analytical Chemistry International Series of Monographs in Analytical Chemistry, 38 Oxford, Pergamon, 1970.